

## Article

# Positively Charged Lipid as Potential Tool to Influence the Fate of Ethosomes

Antonia Mancuso <sup>1</sup>, Maria Chiara Cristiano <sup>2</sup>, Massimo Fresta <sup>1</sup>, Daniele Torella <sup>2</sup> and Donatella Paolino <sup>2,\*</sup>

<sup>1</sup> Department of Health Science, Campus Universitario–Germaneto, University “Magna Græcia” of Catanzaro, Viale Europa, 88100 Catanzaro, Italy; antonia.mancuso@unicz.it (A.M.); fresta@unicz.it (M.F.)

<sup>2</sup> Department of Experimental and Clinical Medicine, Campus Universitario–Germaneto, University “Magna Græcia” of Catanzaro, Viale Europa, 88100 Catanzaro, Italy; mchiara.cristiano@unicz.it (M.C.C.); dtorella@unicz.it (D.T.)

\* Correspondence: paolino@unicz.it; Tel.: +39-0961-3694211

**Abstract:** Ethosomes<sup>®</sup> are one of the main deformable vesicles proposed to overcome the stratum corneum. They are composed of lecithin, ethanol and water, resulting in round vesicles characterized by a narrow size distribution and a negative surface charge. Taking into account their efficiency to deliver drugs into deeper skin layers, the current study was designed to evaluate the influence of different lipids on the physico-chemical features of traditional ethosomes in the attempt to influence their fate. Three lipids (DOPE, DSPE and DOTAP) were used for the study, but only DOTAP conferred a net positive charge to ethosomes, maintaining a narrow mean size lower than 300 nm and a good polydispersity index. Stability and in vitro cytotoxic studies have been performed using Turbiscan Lab analysis and MTT dye exclusion assay, respectively. Data recorded demonstrated the good stability of modified ethosomes and a reasonable absence of cell mortality when applied to human keratinocytes, NCTC 2544, which are used as a cell model. Finally, the best formulations were selected to evaluate their ability to encapsulate drugs, through the use of model compounds. Cationic ethosomes encapsulated oil red o and rhodamine b in amounts comparable to those recorded from conventional ethosomes (over 50%). Results recorded from this study are encouraging as cationic ethosomes may open new opportunities for skin delivery.

**Keywords:** ethosomes; cationic ethosomes; drug delivery systems; surface charge; cutaneous administration



**Citation:** Mancuso, A.; Cristiano, M.C.; Fresta, M.; Torella, D.; Paolino, D. Positively Charged Lipid as Potential Tool to Influence the Fate of Ethosomes. *Appl. Sci.* **2021**, *11*, 7060. <https://doi.org/10.3390/app11157060>

Academic Editor: Nasim Nosoudi

Received: 5 July 2021

Accepted: 29 July 2021

Published: 30 July 2021

**Publisher's Note:** MDPI stays neutral with regard to jurisdictional claims in published maps and institutional affiliations.



**Copyright:** © 2021 by the authors. Licensee MDPI, Basel, Switzerland. This article is an open access article distributed under the terms and conditions of the Creative Commons Attribution (CC BY) license (<https://creativecommons.org/licenses/by/4.0/>).

## 1. Introduction

Over the last few decades, there has been a growing interest in the transcutaneous delivery of active compounds [1–3]. The reason for this interest is mainly related to the numerous advantages offered by this route of administration over traditional oral administration, such as avoiding hepatic first pass metabolism, low risk of systemic side-effects, easy accessibility, and an increase in patient compliance [4]. Although the transcutaneous delivery of active compounds offers many advantages, several drugs are difficult to pass through the main skin barrier, i.e., stratum corneum, due to their chemical–physical properties [5]. For this reason, different strategies have been proposed to improve the permeation of active compounds through the skin barrier, including the use of chemical penetration enhancers, microneedles, laser ablation, and ultrasounds [6–8]. Among all of these, the use of nanosized carriers for cutaneous delivery of drugs seems to offer the best advantages in terms of efficacy and safety of treatment [9,10]. Liposomes are the first proposed nanosized carriers; they are made of biodegradable phospholipids and they are able to deliver both hydrophobic and hydrophilic drugs [11,12]. However, due to their rigid structure, they showed some limits to deliver active compounds into the deeper skin layers [13]. Soon after, it was discovered that the addition of a small amount of so-called “chemical permeation enhancers” in the structure of conventional liposomes led to the realization of deformable

vesicles that were able to more easily permeate through skin layers [14]. Ethosomes<sup>®</sup>, first introduced by Touitou et al. [15] are one of the main known deformable systems for topical use. Ethanol, present in small quantities in their structure, acts as permeation enhancer, reversibly modifying the skin structure [16] to facilitate the passage of active compounds through skin. In detail, Touitou et al. demonstrated that using greater amounts of ethanol during the preparation of the sample, the realization of micellar systems can occur, but in the case of amounts lower than 50% *w/v*, the vesicular bilayered structure was retained [15].

Although deformable vesicles have been shown to be able to increase the transcutaneous penetration of drugs both *in vitro* and *in vivo* [17–20], the influence of surface charge modifications on permeation still represents an open question [20–22]. Indeed, even if the effectiveness of negatively charged liposomal systems has already been reported in many studies [19,23,24], other authors have assumed and demonstrated that the skin permeation of molecules loaded in positively charged vesicles, obtained using, for example, 2-dioleoyl-3-trimethylammonium-propane (DOTAP), was greater than that recorded in the case of negatively charged ones [25,26]. In particular, the electrostatic interaction between positively charged vesicles with skin lipids having negative charge seemed to enhance penetration through skin. An interesting study proposed by Jung and co-workers [27] proved that cationic liposomes were able to reach an average relative penetration depth of around 70% of hair follicle length. In this work, the authors obtained cationic nanosystems made up of dimyristoylphosphatidylcholine, N-(2,3-dioleoyloxy-1-propyl) trimethylammonium methyl sulfate, and cholesterol (50:10:40 mol%), able to interact with negative charge of the hair surface by ion-exchange, reaching an high local concentration. Considering that hair follicles can play the role of reservoir for topically applied molecules, these skin appendages could represent a target of particular interest for transcutaneous delivery of active molecules. For this reason, the great ability of cationic ethosomes to permeate skin through hair follicles needs to be taken into account and further investigated.

The aforementioned hypotheses have prompted us to realize a new system having similar composition with respect to classical ethosomes, already known as good skin permeating systems. Compared to conventional ethosomes, our system contains a small amount of cationic lipids able to confer the positive charge to the vesicular systems. Preliminary characterization studies and the evaluation of the safety of the system have been carried out, thus comparing the results with that obtained from ethosomal systems having a conventional structure. Cationic ethosomes showed suitable properties for topical cutaneous administration, a comparable encapsulation efficiency for model compounds with that recorded from conventional ethosomes. Moreover, they presented good stability over time and great safety properties both *in vitro* and *in vivo*.

For these reasons, the new realized cationic systems appear to be promising for carrying out further permeation studies aimed at elucidating the influence of positively charged surfaces on permeation in deeper skin layers or specific cutaneous compartment, such as follicles, in comparison with the already known ethosomal vesicles.

## 2. Materials and Methods

### 2.1. Materials

Phosphatidylcholine (Phospholipon<sup>®</sup> 90 G, PL90G) was supplied by Lipoid GmbH (Ludwigshafen, Germany); 1,2-dioleoyl-sn-glycero-3-phosphoethanolamine (DOPE), 1,2-dioleoyl-3-trimethylammonium-propane (DOTAP) and 1,2-Distearoyl-sn-glycero-3-phosphorylethanolamine (DSPE) were purchased from Avanti Polar Lipids. NCTC2544 cells were provided by Istituto Zooprofilattico di Modena e Reggio Emilia (Reggio Emilia, Italy). Dulbecco's Modified Eagle's Medium (D-MEM), trypsin/EDTA (ethylenediaminoacetic acid) solution and fetal bovine serum (FBS) were obtained from GIBCO (Invitrogen Corporation, Milan, Italy). Solution of amphotericin B (250 µg/mL), phosphate buffer saline solution (PBS) and 3-[4,5-dimethylthiazol-2-yl]-3,5-diphenyltetrazolium bromide (MTT) salts were purchased from Sigma-Aldrich (Milan, Italy). All substances and solvents (Carlo Erba,

Milan, Italy) used for experiments were of high analytical grade and did not require further purification processes.

## 2.2. Preparation of Samples

Ethosome colloidal suspension was prepared as previously described by Touitou et al. with slight modifications [15,16], using specific lipidic mixtures (1% *w/v*). Briefly, Phospholipon® 90 G was solubilized in ethanol (40% *w/v*) using a hermetically sealed Pyrex® glass vial. Double distilled water (59% *w/v*) was added dropwise at room temperature to the lipidic solution through an injection system connected to the perforated cup of the vial. This strategy allowed to reduce the evaporation of ethanol as much as possible. The obtained formulation was homogenized using Ultra-Turrax T25 equipped with a S25 N-8G homogenizing probe (IKA WERKE GMBH and Co., Staufen, Germany) for 1 min at 15,000 rpm and maintained at room temperature for 30 min before analysis. Using this protocol, the amount of free ethanol was evaporated and structural ethanol was retained over time. Table 1 shows the lipid composition of the different ethosomal formulations realized for this study. Conventional ethosomes, made of only Phospholipon® 90 G (PL 90 G, 1% *w/v*), ethanol (40% *w/v*) and water (59% *w/v*), were obtained (formulation A) and used as control. Ethosomes having different lipidic composition (1% *w/v*) were prepared using a mixture of PL 90 G and other lipids, having positive charges in their structure (DOPE, DOTAP or DSPE), at different molar ratios (formulations B-M).

**Table 1.** Lipid composition of different ethosomal formulations prepared for the study.

Formulation	Lipid Composition	
	Lipidic Mixture	Molar Ratio
A	PL90G <sup>1</sup>	-
B	PL90G:DSPE <sup>2</sup>	10:1
C	PL90G:DOPE <sup>3</sup>	10:1
D	PL90G:DOTAP <sup>4</sup>	10:1
E	PL90G:DOTAP	10:2
F	PL90G:DOTAP	10:3
G	PL90G:DOTAP	10:4
H	PL90G:DOTAP	10:5
I	PL90G:DOTAP	10:0.5
J	PL90G:DOTAP	10:0.4
K	PL90G:DOTAP	10:0.3
L	PL90G:DOTAP	10:0.2
M	PL90G:DOTAP	10:0.1

<sup>1</sup> Phospholipon® 90 G. <sup>2</sup> 1,2-Distearoyl-sn-glycero-3-phosphorylethanolamine. <sup>3</sup> 1,2-Dioleoyl-sn-glycero-3-phosphoethanolamine. <sup>4</sup> 1,2-Dioleoyl-3-trimethylammonium-propane.

To achieve probe-loaded vesicles, 100 µg/mL of rhodamine, red oil and bromophenol blue salt were added during the preparation of samples and respectively used as hydrophilic, lipophilic, and amphiphilic model compounds.

## 2.3. Physico-Chemical Characterization of Vesicles

The dynamic light scattering spectrophotometer, Zetasizer Nano ZS (Malvern Instruments Ltd., Worcestershire, UK) was used to investigate the mean size, polydispersity index and surface charge of the realized nanocarriers. Before analysis, each sample was diluted in aqueous medium to avoid multiscattering phenomena. Measures were performed on three different batches of each sample and results of analysis were reported as the mean of three measurements (each one of 10 determinations) ± standard deviations.

The stability of each formulation was also investigated using Turbiscan® Lab (Formulation, L'Union, France). In detail, a pulsing near infrared LED set at 880 nm crossed a cylindrical glass vial containing the formulation in the whole height and the light flux transmitted (T) and backscattered (BS) by the sample was recorded as a relative percentage

referred to a suspension of polystyrene latex and silicone oil, used as standards. Measurements were recorded for 3 h at  $24 \pm 1$  °C and data were processed by Turbiscan Easy Soft Converter (Formulation, L'Union, France) [28]. The stability kinetics of the realized sample was also calculated through the evaluation of their Turbiscan Stability Index (TSI) and the obtained profiles were compared to each other.

To further investigate the long-term stability of samples, formulations were sealed in an amber glass vial and carefully stored at +4 °C for 1 month. At the end of this period, each sample was properly vortexed, a macroscopic analysis was done and characterization studies were repeated to investigate any changes that occurred in the realized samples.

#### 2.4. Cell Cultures

Cytotoxic effect of ethosomal formulations were investigated on human keratinocytes, NCTC2544 cells, through the MTT (3-[4,5-dimethylthiazol-2yl]-2,5-diphenyltetrazoliumbromide) dye assay, collecting data of cell viability. Cells were seeded in Petri dishes ( $\varnothing$  100 × 20 mm) containing minimum essential medium (D-MEM) supplemented with glutamax, streptomycin (100 µg/mL)–penicillin (100 µL/mL) solution (1% *v/v*), amphotericin B (250 µg/mL), and FBS (10% *v/v*) and stored in a Water-Jacketed CO<sub>2</sub> incubator at a temperature of 37 °C. Medium was replaced every two days until a confluence of ~80% was reached. Cells were then washed with phosphate buffer solution, treated with trypsin/EDTA (1X) solution to be detached from the dishes and transferred into centrifuge tubes. Tubes were centrifuged at  $1200 \times g$  rpm for 5 min using Megafuse 1.0 (Heraeus Sepatech, Osterode, Germany) obtaining a pellet that was resuspended in D-MEM [22].

#### Evaluation of Cytotoxicity on NCTC2544 Cells

NCTC2544 cells were seeded in 96-well plastic culture dishes at a density of  $5.0 \times 10^3$  cells/0.1 mL to perform MTT dye test as previously reported [22]. Following 24 h of incubation, D-MEM was replaced with a fresh medium containing empty ethosomes at increasing concentration of lipidic components (0.01, 0.1, 1.0 and 10.0 µg/mL). Cells were incubated for different times (24 h, 48 h and 72 h), treated with 10 µL of MTT solution (5 mg/mL of salts dissolved in PBS buffer) and further incubated at 37 °C and 5% CO<sub>2</sub> for 3 h, which was the time necessary to living cells to form violet formazan crystals. At this time, culture medium was withdrawn and formazan crystals were dissolved in dimethylsulfoxide/ethanol (1:1 *v/v*), keeping the plate under constant stirring using IKA® KS 130 Control (IKA® Werke GmbH & Co., Staufen, Germany) for 20 min at 200 rpm. ELISA microplate reader (Labsystems mod. Multiskan MS, Midland, ON, Canada) set at  $\lambda_{exc}$  570 nm and  $\lambda_{em}$  670 nm, allowed to investigate cell viability according to the following equation:

$$\% \text{ Cell viability} = \frac{A_t}{A_u} \cdot 100 \quad (1)$$

where  $A_t$  and  $A_u$  represented the absorbance of treated and untreated cells, respectively. Three different experiments were performed to investigate the percentage of cell viability and results were reported as the average of the obtained data  $\pm$  standard deviation.

#### 2.5. Evaluation of Entrapment Efficiency

The entrapment efficiency of probe-loaded nanovesicles was determined following the ultracentrifugation of samples. Ethosomes were transferred in polycarbonate tubes and centrifuged for 1 h at 4 °C and  $85,000 \times g$  rpm using an Avanti 30 centrifuge (Beckman, Fullerton, CA, USA). The supernatant was separated from the pellet and collected to be analyzed using high performance liquid chromatography (HPLC) apparatus (Varian Inc., Palo Alto, CA, USA). The entrapment efficiency of the systems was found according to the following equations:

$$EE(\%) = \left[ \frac{(D_t - D_s)}{D_t} \right] \cdot 100 \quad (2)$$

$$EE(\%) = \left[ \frac{(De)}{Dt} \right] \cdot 100 \quad (3)$$

where  $Dt$  was the amount of probe used during the preparation of samples,  $Ds$  and  $De$  were, respectively, the amounts of probe recorded in the supernatant and pellet [22]. The two equations reported very similar values that differed by less than 2%.

### HPLC Analysis

The content of the probe loaded into the systems was determined using HPLC system carrying out the separation at room temperature with a GraceSmart RP C18 column with  $4.6 \times 250$  mm,  $5 \mu\text{m}$  particle size (Alltech Grom GmbH, Rottenburg-Hailfingen, Germany). The HPLC system was equipped with a 200-2031 Metachem online degasser, a binary pump M210, a G1316A thermostatted column compartment, a ProStar 410 autosampler and a  $25 \mu\text{L}$  CSL20 Cheminert Sample Loop injector. A mixture of water/methanol (80:20  $v/v$ ) was used as mobile phase at a flow rate of 1.0 mL/min and UV detection was set at 592 nm, 359 nm and 543 nm, respectively, for bromophenol blue, oil red o and rhodamine. Data were processed using Galaxie<sup>®</sup> chromatography manager software (Varian Inc., Palo Alto, CA, USA).

### 2.6. In Vivo Tolerability Studies

In vivo studies were performed on healthy human volunteers using X-Rite SP60 portable sphere spectrophotometer (X-Rite Incorporated, Grandville, MI, USA), which represents a colorimeter able to detect any changes in skin color [19]. Six volunteers were broadly informed about the procedures and the aim of the study and gave their written consent to participate. The experimental protocol provided that all subjects enrolled in the study rested under room conditions ( $22 \pm 3$  °C and 40–50% relative humidity) for 30 min before starting with the study. Four sites (each one  $1 \text{ cm}^2$ ) were outlined on the ventral surface of both forearms of each volunteer and baseline values of erythema index (E.I.) were recorded before applying the samples. Hill Top chambers (Hill Top Research, Inc. Cincinnati, Miami, OH, USA) were filled with 1 mL of each sample and applied to the defined sites. Saline solution (0.9%  $w/v$  NaCl) was applied on one site as control, the other sites were treated with conventional ethosomes and ethosomes made of Phospholipon 90 G:DOTAP at increasing concentrations (10:0.5 and 10:1, molar ratio). Data were reported as the variation of erythema index ( $\Delta\text{E.I.}$ ) values following treatment with samples compared to baseline values. The induced erythema was monitored over 6 h, 24 h and 48 h, considering the following equation:

$$\text{E.I.} = 100 \left[ \log \frac{1}{R560} + 1.5 \left( \log \frac{1}{R540} + \log \frac{1}{R580} \right) - 2 \left( \log \frac{1}{R510} + \log \frac{1}{R610} \right) \right] \quad (4)$$

where E.I. represents the erythema index;  $1/R$  is the inverse reflectance at the wavelength corresponding to the relative absorption peaks of hemoglobin ( $\lambda = 540 \text{ nm}$ ;  $\lambda = 580 \text{ nm}$ ;  $\lambda = 560 \text{ nm}$ ) and melanin ( $\lambda = 510 \text{ nm}$  and  $\lambda = 610 \text{ nm}$ ).

### 2.7. Statistical Analysis

One-way ANOVA test and Bonferroni test were used to investigate the statistical significance. The minimal value of significance for all experiments was set to  $p < 0.05$ .

## 3. Results and Discussion

### 3.1. Physico-Chemical Characterization Studies

A deeper investigation of the physico-chemical and technological formulation properties of a new drug delivery system represents both a fundamental and limiting step for the realization of an eligible formulation. The suitability of a nanocarrier for a specific administration route depends on different parameters. Indeed, mean sizes, size distribution, any surface charge and the stability of a sample over time are important factors that influence

the pharmacokinetics of the realized system [26,29,30]. Especially in the case of cutaneous administration, these parameters are essential to define the permeation of the carrier or any delivered substance [20,31,32].

In this study, a new carrier for topical cutaneous administration was realized and characterized, taking into account the conventional composition of ethosomes, a well-known drug delivery system having advantageous properties for cutaneous administration [15]. The realization of the new system was made in the attempt to maintain the ability of conventional ethosomes to be used as skin drug delivery systems, modifying their surface charge to influence their fate. Conventional ethosomes owe their ability to permeate through the skin barrier to the elasticity conferred by the presence of ethanol in their structure [33,34]. Moreover, data reported in the literature often showed a correlation between ethosomal size and the amount of lipids and ethanol in their structure. In particular, sizes of ethosomes decrease as the concentration of ethanol increases and soybean phosphatidylcholine decreases [15,35]. Since size represents a very important feature for topical drug delivery systems, we chose conventional ethosomes with minimum amount of phospholipon 90G (1% *w/v*) and a high amount of ethanol (40% *w/v*) to propose this system as the control for our further studies. The threshold of 40% *w/v* ethanol was not exceeded because, as previously reported, these systems showed a certain instability in the presence of an amount of 45% *w/v* ethanol [36]. Analysis of dynamic light scattering was performed using Zetasizer Nano ZS and results, reported in Table 2, showed a narrow size distribution with dimensions lower than 300 nm for the conventional ethosomal (formulation A), thus indicating that they were small enough for topical administration and transcutaneous passage [37]. Ethosomes having conventional composition, also reported a net negative surface charge, which is essential to avoid aggregation phenomena and to ensure a good stability of sample over time [38]. The stability of conventional ethosomes was further investigated using Turbiscan Lab<sup>®</sup>. Results of  $\Delta$ Transmission and  $\Delta$ Backscattering showed good stability profiles, within a range of  $\Delta$ Backscattering  $\pm 1$  (see Supplementary Materials, Figure S1), thus confirming the results obtained in one of our previous studies [36].

**Table 2.** Physico-chemical properties of conventional and positive charged ethosomes.

Formulation	Mean Size (nm)	Polydispersity Index	Zeta Potential (mV)
A	224 $\pm$ 3	0.16 $\pm$ 0.01	−25 $\pm$ 0
B	208 $\pm$ 1	0.20 $\pm$ 0.02	−24 $\pm$ 1
C	241 $\pm$ 5	0.23 $\pm$ 0.02	−27 $\pm$ 1
D	152 $\pm$ 2	0.16 $\pm$ 0.02	+56 $\pm$ 1

In fact, the ability of conventional ethosomes to interact with skin lipids and to improve the permeation of any delivered drug has been widely studied [16,36,39]. However, due to recent and conflicting discoveries concerning the influence of the surface charge on the transdermal flux and direction of delivered drugs [22,26], new vesicular systems have been realized using three different lipids having positive charges in their structures, with the aim to investigate how much they influence the behavior of ethosomes. In this attempt, the first step regarded the design and characterization of a cationic ethosomal formulation. The composition of formulation A was retained and the amount of PL<sup>®</sup>90 G was replaced with the same amount of a lipidic mixture between PL<sup>®</sup>90G and lipids with positive charge (10:1, molar ratio). As can be seen in Table 2, formulations B and C, which respectively, contained DSPE and DOPE, showed no relevant variations in the physico-chemical properties of the samples, if compared to the results recorded for formulation A, because all had a net negative surface charge and a narrow size distribution with vesicular dimensions below 250 nm. On the contrary, the addition of DOTAP to the sample at the same molar ratio (formulation D) led to a clear change in the surface charge of the nanosystems, which converted to a net positive charge.

Probably, the persistence of the negative surface charge for formulations B and C was due to the positioning of lipid in the bilayer, which induced masking of the positive

functional groups of lipid molecules. Moreover, the simultaneous presence of phosphate groups in DSPE and DOPE, which on the contrary was missing in DOTAP, could have counterbalanced the positive charge and strongly influenced the final surface charge of nanovesicles.

Compared to formulation A, a reduction in vesicle sizes occurred in the case of formulation D, probably due to a better packing between the fraction of lipidic constituents having opposite charge. The low value of polydispersity index recorded in the case of formulation D also confirmed that the narrow distribution was retained by the new realized system, compared to conventional ethosomes. Moreover, the low value of polydispersity index and the net surface charge suggested a good stability of the system [40].

The great stability of the obtained cationic ethosomes (formulation D) was further confirmed by investigating  $\Delta$ Transmission and  $\Delta$ Backscattering profiles over 3 h using Turbiscan Lab<sup>®</sup>. As can be seen in Figure 1,  $\Delta$ Backscattering profiles were within the range of  $\pm 1\%$ , indicating that no creaming, sedimentation and flocculation phenomena occurred during the analysis, suggesting a great stability of samples over time. Any positive and negative variations in backscattering profiles over 8 mm and under 2 mm, that are visible in Figure 1, were not related to destabilization phenomena but were dependent on enclosed air, respectively, at the top and bottom of the glass vial [41].

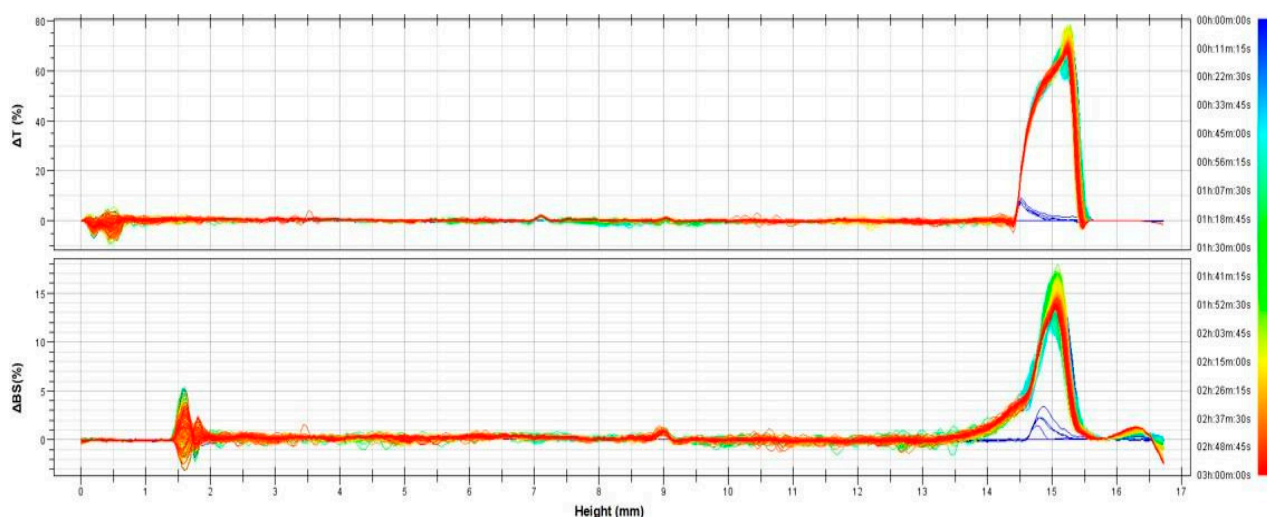


**Figure 1.** Delta transmission ( $\Delta T$ ) and delta backscattering ( $\Delta BS$ ) profiles of cationic ethosomes made of Phospholipon 90G and DOTAP (10:1 molar ratio). The figure is representative of three different experiments performed for the sample. Data are reported as a function of time (0–3 h) and sample height (mm).

### 3.2. Characterization of Cationic Vesicles Made of Different Amount of DOTAP

Starting from the interesting results obtained for formulation D, further investigations were performed to test the influence of variable amounts of DOTAP in the main features of the sample and to find the best concentration to be used for subsequent *in vitro* and *in vivo* studies. For this reason, the concentration of cationic lipid, expressed as molar ratio (PL90 G:DOTAP) was both progressively increased (formulations E–H) and reduced (formulations I–M) compared to the amount reported for formulation D (PL90G:DOTAP, 10:1) and further characterization studies have been performed using Zetasizer Nano ZS. As can be seen in Table 3, the increase in DOTAP amount led to an increase in vesicle sizes. Polydispersity index values also increased compared to that recorded from formulation D and this was probably due to the simultaneous formation of micellar systems following the accumulation of lipids that were not structured in the carrier [42]. The mean sizes of vesicles also increased, overcoming 500 nm in size, which was too high a value to consider these carriers for topical cutaneous administration [37].

On the other hand, the reduction in the amount of DOTAP used during the preparation of formulations I-M showed good values of size and polydispersity index, but a gradual reduction in the net positive surface charge of the vesicles congruent with a reduction in the amount of positive lipid added during the preparation of samples. The increase in the zeta potential values towards more positive values as a function of the increasing amount of DOTAP added confirmed that the cationic lipid molecules were disposed on the surface of the nanovesicles. Despite the reduction of zeta potential values related to the reduction in the addition of cationic lipids, all investigated samples showed values beyond the threshold of +30 mV, commonly considered suitable for guaranteeing repulsion between vesicles thus avoiding aggregation phenomena [40].

**Table 3.** Characterization studies of ethosomes containing DOTAP and phospholipon® 90 G at different molar ratios. The generic composition of formulation B was maintained, considering the final amount of 1% *w/v* of lipids, 40% *w/v* of ethanol and 59% *w/v* of water.

Formulation	Lipid Composition		Size (nm)	Polydispersity Index	Zeta Potential (mV)
	Lipidic Mixture	Molar Ratio			
E	PL90G:DOTAP	10:2	274 ± 2	0.40 ± 0.01	+55 ± 1
F	PL90G:DOTAP	10:3	505 ± 22	0.41 ± 0.08	+58 ± 3
G	PL90G:DOTAP	10:4	512 ± 9	0.27 ± 0.02	+64 ± 1
H	PL90G:DOTAP	10:5	616 ± 16	0.32 ± 0.06	+69 ± 1
I	PL90G:DOTAP	10:0.5	189 ± 2	0.13 ± 0.01	+52 ± 1
J	PL90G:DOTAP	10:0.4	141 ± 1	0.19 ± 0.01	+50 ± 0
K	PL90G:DOTAP	10:0.3	198 ± 2	0.14 ± 0.01	+47 ± 3
L	PL90G:DOTAP	10:0.2	216 ± 4	0.25 ± 0.02	+47 ± 2
M	PL90G:DOTAP	10:0.1	301 ± 2	0.20 ± 0.02	+42 ± 1

In fact, the values needed to avoid destabilizing phenomena are questioned due to the great influence of several other parameters to be considered, such as the solvent used, the concentration of ions, and functional groups of the surface [40]. For this reason, further stability studies have been performed. The stability kinetics profiles of all cationic ethosomes (formulations D-M) were investigated using Turbiscan Lab analysis and the results were compared. As can be seen in Figure 2, the addition of different amounts of DOTAP did not result in a marked variation of TSI values compared to those recorded for formulation D, which also reported  $\Delta T$  and  $\Delta BS$  profiles within an excellent stability range (Figure 2). These results suggested that no relevant instability phenomena were to be expected for the analyzed samples.

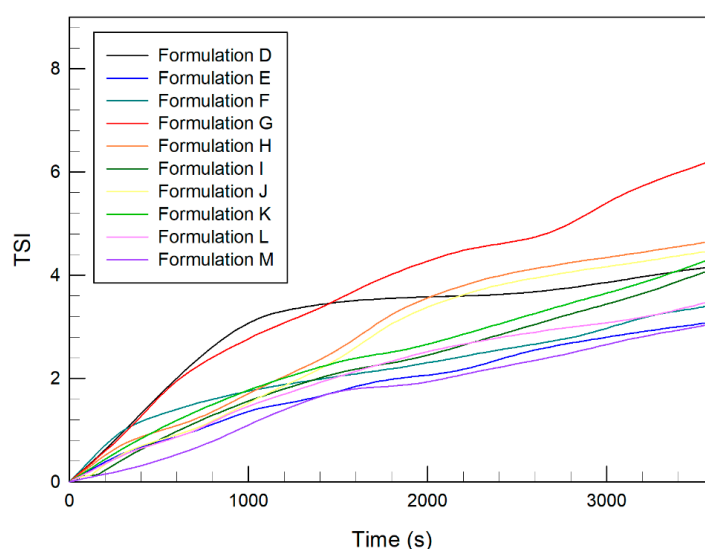


**Figure 2.** Kinetic stability profiles of cationic ethosomes using Turbiscan Lab® Expert. The results are representative of three independent analyses of samples performed at 25 °C for 1 h.

Another stability test was performed, incubating samples at 4 °C for 1 month, mimicking a conservation process, and then evaluating any changes in their sizes and polydispersity index. It is interesting to note that no marked variations occurred over time in any samples (Figure 3). This was a desirable feature because, once again, the great stabilization of the nanovesicles provided by the addition of lipids with positive charge was confirmed.

As can be seen in Figure 3, formulations D, E, I, J, K, and L retained sizes lower than 300 nm after 1 month of incubation. Between them, formulation D and formulation I also reported the best values of polydispersity (lower than 0.2) after 1 month of incubation.

The previously described results of physicochemical characterization studies allowed us to choose the most suitable profiles. In particular, the two samples with lower mean sizes, higher positive surface charges (formulation D and formulation I) and good stability profiles over 1 month were considered for further studies.

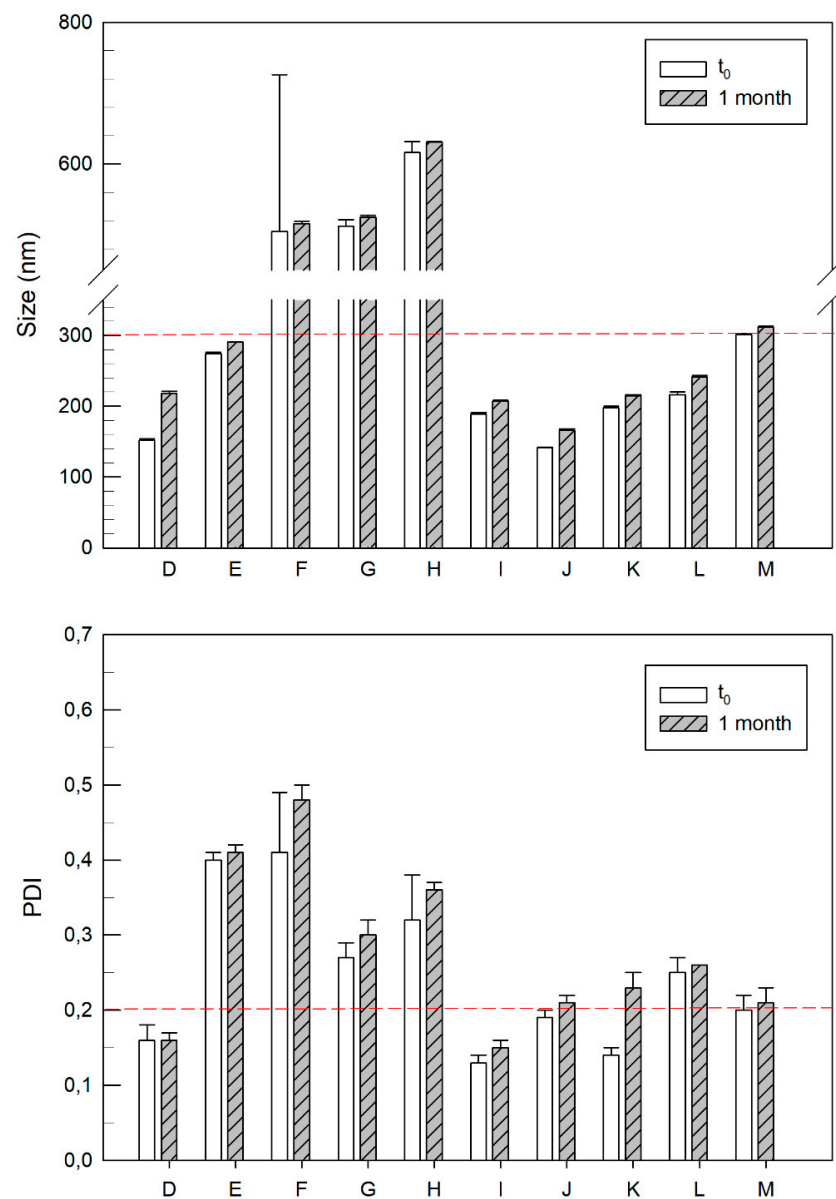


**Figure 3.** Characterization studies of ethosomes containing positive lipids and Phospholipon® 90 G at different molar ratios, after their storage at 4 °C, for up to 1 month. The dashed red lines delimit the best results recorded in terms of size and polydispersity index (below the line). Results are expressed as mean values of three different experiments  $\pm$  standard deviation.

### 3.3. In Vitro Cytotoxicity Studies

The in vitro bioassay was performed on human keratinocytes (NCTC-2544 cells) to investigate if the inclusion of DOTAP in ethosomal systems affected cell viability. It is well known that cationic lipids improve transfection [43] due to the increase in electrostatic interactions between cellular membranes and vesicles but it is noteworthy that this could influence cell viability. To further investigate this aspect, in vitro studies were performed.

The non-differentiated keratinocytes cell line was chosen as a model, assuming a cutaneous topical administration of the realized samples. NCTC-2544 cells were treated with different vesicular formulations at increasing concentrations with reference to lipidic amounts (0.01, 0.1, 1.0 and 10.0  $\mu\text{g}/\text{mL}$ ) for 24 h, 48 h and 72 h.

As can be seen in Figure 4, all samples tested, i.e., conventional ethosomes, formulation D and formulation I, showed appropriate safety, thus indicating a good biocompatibility of the realized samples, with keratinocytes cells up to lipid concentrations of 10  $\mu\text{g}/\text{mL}$ , as the cell viability was found above 70% within 72 h.

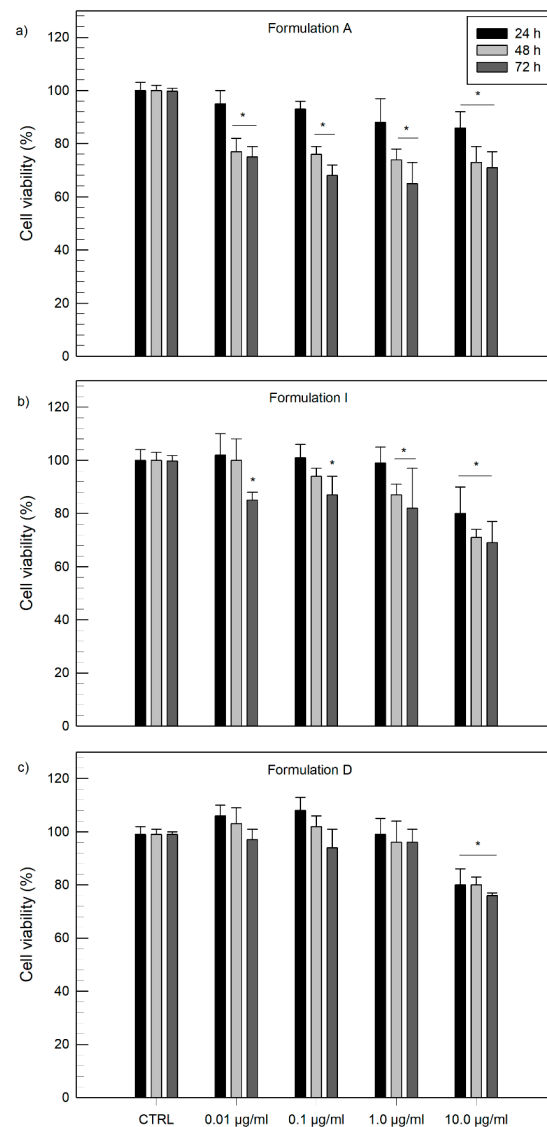


**Figure 4.** Evaluation of cytotoxicity of ethosomal systems on NCTC-2544 cells through MTT test after 24 h, 48 h and 72 h of treatment. Conventional ethosomes, formulation A (a), ethosomes made of PL90G:DOTAP 10:0.5 molar ratio, formulation I (b) and ethosomes PL90G:DOTAP 10:1 molar ratio, formulation D (c) have been used for this study. Results are expressed as the mean value of three different experiments  $\pm$  standard deviation. \*  $p$  value  $< 0.05$  with respect to control (untreated cells).

Previous studies in the literature reported that cationic lipids with ester bonds in the linker zone, such in the case of DOTAP, showed less cytotoxic effects in cultured cells [44–46]. Surprisingly, in this study, cationic ethosomes made of DOTAP at a 10:0.5 molar ratio (Figure 4b) and 10:1 molar ratio (Figure 4c), not only showed low cytotoxic effects, but they also seemed to show great safety profiles on NCTC 2544 cells at 72 h until a lipid concentration of 1.0 µg/mL when compared to profiles recorded from conventional ethosomal samples (Figure 4a).

### 3.4. Evaluation of Encapsulation Efficiency

The ability of formulations D and I to encapsulate active compounds was also investigated by adding oil red O, rhodamine B or bromophenol blue salt as lipophilic, hydrophilic, and amphiphilic model drugs, respectively. First of all, further characterization studies have been performed to investigate the mean sizes, zeta potential and the stability of samples to assess whether they suffered significant changes and if they retained their suitability for topical use. It was interesting to note that in any case the addition of a probe, regardless of their chemical properties, caused a significant ( $p < 0.001$ ) reduction in vesicle sizes (Table 4), probably related to a rearrangement of the structure of the carrier. A slight increase in the polydispersity index values was recorded for the addition of oil red o, despite all values remaining below an acceptable threshold [47]. As in the case of the charge of cationic ethosomes (formulations D and I), a reduction of values was recorded proportionally to the reduction in size compared to empty formulations. Nevertheless, carriers loaded with one of the three probes still retained a net positive surface charge that was proportional to the amount of cationic lipid added during preparation. The stability of each sample was checked using Turbiscan Lab analysis (Figure S2). Formulations showed good stability profiles reporting  $\Delta$ Backscattering values in a range of  $\pm 1$  for any probe added in conventional ethosomes (Figure S2A) or into cationic ethosomal systems (Figure S2B,C) thus confirming that no creaming, flocculation or sedimentation phenomena occurred by the addition of model compounds into the realized systems.

**Table 4.** Physico-chemical properties of conventional ethosomes (formulation A) and positive charged ethosomes (formulations D and I) loaded with probes. Oil red o, rhodamine and bromophenol blue were used, respectively, as lipophilic, hydrophilic or amphiphilic model compounds.

Dye	Formulation	Mean Size (nm)	Polydispersity Index	Zeta Potential (mV)	Encapsulation Efficiency (%)
Oil red O	A	100 ± 1	0.19 ± 0.02	−25 ± 1	43 ± 3
	D	112 ± 3	0.29 ± 0.01	+38 ± 2	55 ± 2
	I	105 ± 1	0.33 ± 0.01	+29 ± 3	50 ± 2
Rhodamine B	A	132 ± 2	0.17 ± 0.02	−14 ± 1	69 ± 4
	D	108 ± 2	0.13 ± 0.01	+33 ± 2	52 ± 2
	I	118 ± 1	0.08 ± 0.01	+31 ± 1	69 ± 6
Bromophenol blue	A	88 ± 3	0.18 ± 0.01	−16 ± 1	27 ± 2
	D	94 ± 2	0.16 ± 0.00	+28 ± 2	15 ± 6
	I	135 ± 2	0.08 ± 0.02	+13 ± 2	36 ± 3

The new realized cationic systems also showed good abilities to encapsulate hydrophilic and lipophilic probes (above 50% of the amount added during the phase of preparation), comparable with those recorded from well-known drug delivery systems, i.e., conventional ethosomes [15,34,36]. In detail, formulations D and I seemed to encapsulate oil red o better than conventional ethosomes, probably due to a greater interaction between the hydrophobic model compound and the cationic lipid, i.e., DOTAP. Concerning the addition of rhodamine B, conventional ethosomes (formulation A) and cationic ethosomes made of PL90G:DOTAP 10:0.5 molar ratio (formulation I), reported very similar values, while a slight decrease was recorded for an increased amount of DOTAP (formulation D, 10:1 molar ratio). This effect was probably due to a greater bulky effect on the part

of the lipid to the detriment of the aqueous core where the hydrophilic probe is likely to accumulate. Finally, regarding the addition of amphiphilic molecules, such as bromophenol blue, a drastic reduction of the amount encapsulated was recorded for both cationic and conventional ethosomes and once again this amount was lower for increasing amounts of DOTAP in the sample.

### 3.5. In Vivo Human Skin Tolerability Test

The in vivo tolerability of the newly realized systems was tested, monitoring the variation of erythema index values before and following the treatment with ethosomal formulations ( $\Delta E.I.$ ). The obtained values were compared with those recorded following the administration of conventional ethosomes or the administration of saline solution (0.9% NaCl), used as control. The study was performed on six healthy human volunteers over 48 h and the results are reported as the mean of the values recorded  $\pm$  standard deviation.

As can be seen in Figure 5, six hours after the administration of the samples (both conventional ethosomes and cationic formulations), a slight increase in  $\Delta E.I.$  values was recorded. Although the increase was slight, it was significant ( $p < 0.05$ ) if compared to values recorded for the administration of saline solution. This increase in E.I. value was probably related to the permeating ability of ethosomal systems through skin and was consistent with data reported in another study [16]. In particular, the amount of ethanol, which remained unchanged between conventional and cationic ethosomes, probably caused a temporary and reversible modification of the main skin barrier, leading to increasing values of E.I. in the first 6 h. After 24 h values of erythema index were in line with that recorded from saline solution, used as control, meaning that the erythema resolved. Actually, the initial increase of erythema index values due to a reorganization of the skin barrier structure represents an attractive property as this effect can accompany the permeation of any delivered drug through skin layers.

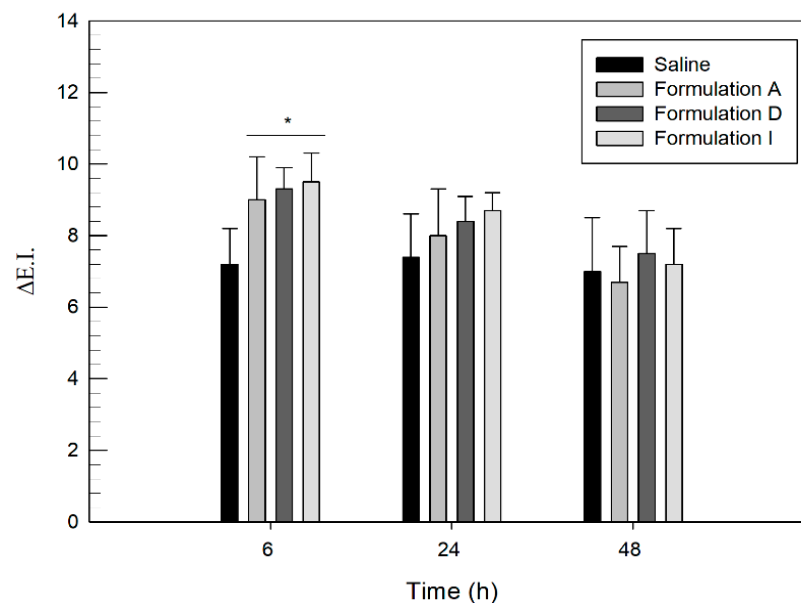


**Figure 5.** Variation of erythema index ( $\Delta E.I.$ ) over 6, 24 and 48 h of treatment with saline solution, formulation A, formulation D and formulation I. Results are expressed as the mean value of six independent experiments  $\pm$  standard deviation. \*  $p$  value  $< 0.05$  compared to saline solution, used as control.

The results obtained from in vivo studies showed suitable levels of cutaneous tolerability and safety of the new realized cationic systems, thus confirming they represent promising systems for topical skin delivery.

#### 4. Conclusions

The role of cationic charges on vesicular systems represents a new trend for topical delivery of active compounds, which needs to be better clarified. In this attempt cationic ethosomal systems made with small amounts of cationic lipids have been realized in this study and compared with data recorded from conventional ethosomal formulations.

The results obtained showed that the addition of small quantities of DOTAP to conventional ethosomes allows to realize positively charged systems. In detail, the systems made of PL90G: DOTAP 10: 1 or 10: 0.5 molar ratio proved to be the most suitable for a possible topical skin application. In our physico-chemical and technological formulation studies, these systems showed average sizes below 300 nm, a low polydispersity index (below 0.2) and a net positive surface charge (over +50 mV) conferring a certain stability to the system. Further characterization studies performed using Turbiscan Lab analysis confirmed the stability of the realized formulations, thus recording values of  $\Delta$ Backscattering within  $\pm 1$ . The storage of samples over one month also confirmed the great stability of the realized samples as no marked variations in size and polydispersity index occurred during this period. Cationic ethosomes presented good encapsulation efficacy of hydrophilic and lipophilic model compounds, comparable to that recorded from conventional ethosomes. In detail, the encapsulation of oil red o or rhodamine b was found to be above 50% of the amount added during the preparation. Toxicity studies carried out on NCTC2544 cells and on healthy volunteers finally proved the suitability of these systems for cutaneous application as they were able to maintain cell viability above 70% within 72 h. Concerning preparation made of DOTAP (10:0.5 and 10:1 molar ratio) they also reported great safety profiles on NCTC 2544 cells at 72 h over lipid concentration of 1.0  $\mu\text{g}/\text{mL}$ . Finally, no relevant irritation phenomena occurred after 48 h from their application to the forearm of healthy human volunteers.

Thus, we can conclude that cationic ethosomes made of PL90G:DOTAP at a 10:1 molar ratio and 10:0.5 molar ratio represent promising systems for further permeation studies, which will allow us to investigate the influence of surface charge on the fate of such deformable systems.

**Supplementary Materials:** The following are available online at <https://www.mdpi.com/article/10.3390/app11157060/s1>, Figure S1: Delta transmission ( $\Delta T$ ) and delta backscattering ( $\Delta BS$ ) profiles of conventional ethosomes (formulation A). Figure S2: Delta transmission ( $\Delta T$ ) and delta backscattering ( $\Delta BS$ ) profiles of probe-loaded ethosomal formulations.

**Author Contributions:** Conceptualization, D.P.; methodology, D.P. and M.F. investigation, A.M. and M.C.C.; data curation, A.M. and D.T.; writing—original draft preparation, A.M.; writing—review and editing, M.C.C.; supervision, D.P. All authors have read and agreed to the published version of the manuscript.

**Funding:** This research received no external funding.

**Institutional Review Board Statement:** The study was conducted according to the guidelines of the Declaration of Helsinki and approved by the Ethics Committee of the Magna Græcia University of Catanzaro (protocol code 391 of 19 December 2019).

**Informed Consent Statement:** Informed consent was obtained from all subjects involved in the study.

**Data Availability Statement:** The data presented in this study are available on request from the corresponding author.

**Conflicts of Interest:** The authors declare no conflict of interest.

#### References

1. Lee, H.; Song, C.; Baik, S.; Kim, D.; Hyeon, T.; Kim, D.H. Device-assisted transdermal drug delivery. *Adv. Drug Deliv. Rev.* **2018**, *127*, 35–45. [[CrossRef](#)]
2. Leppert, W.; Malec-Milewska, M.; Zajaczkowska, R.; Wordliczek, J. Transdermal and topical drug administration in the treatment of pain. *Molecules* **2018**, *23*, 681. [[CrossRef](#)]

3. Krishnan, V.; Peng, K.; Sarode, A.; Prakash, S.; Zhao, Z.; Filippov, S.K.; Todorova, K.; Sell, B.R.; Lujano, O.; Bakre, S.; et al. Hyaluronic acid conjugates for topical treatment of skin cancer lesions. *Sci. Adv.* **2021**, *7*, eabe6627. [[CrossRef](#)] [[PubMed](#)]
4. Antimisiaris, S.G.; Marazioti, A.; Kannavou, M.; Natsaridis, E.; Gkartziou, F.; Kogkos, G.; Mourtas, S. Overcoming barriers by local drug delivery with liposomes. *Adv. Drug Deliv. Rev.* **2021**, *174*, 53–86. [[CrossRef](#)]
5. Prausnitz, M.R.; Elias, P.M.; Franz, T.J.; Schmuth, M.; Tsai, J.-C.; Menon, G.K.; Holleran, W.M.; Feingold, K.R. Skin Barrier and Transdermal Drug Delivery STRUCTURE AND ORIGIN OF THE SKIN BARRIER Stratum Corneum Structure and Organization. *Med. Ther.* **2012**, *124*, 2065–2073.
6. Lee, W.R.; Shen, S.C.; Aljuffali, I.A.; Li, Y.C.; Fang, J.Y. Impact of different vehicles for laser-assisted drug permeation via skin: Full-surface versus fractional ablation. *Pharm. Res.* **2014**, *31*, 382–393. [[CrossRef](#)] [[PubMed](#)]
7. Kováčik, A.; Kopečná, M.; Vávrová, K. Permeation enhancers in transdermal drug delivery: Benefits and limitations. *Expert Opin. Drug Deliv.* **2020**, *17*, 145–155. [[CrossRef](#)]
8. Kirkby, M.; Hutton, A.R.J.; Donnelly, R.F. Microneedle Mediated Transdermal Delivery of Protein, Peptide and Antibody Based Therapeutics: Current Status and Future Considerations. *Pharm. Res.* **2020**, *37*, 117. [[CrossRef](#)]
9. Singh Malik, D.; Mital, N.; Kaur, G. Topical drug delivery systems: A patent review. *Expert Opin. Ther. Pat.* **2016**, *26*, 213–228. [[CrossRef](#)]
10. Liakopoulou, A.; Mourelatou, E.; Hatziantoniou, S. Exploitation of traditional healing properties, using the nanotechnology's advantages: The case of curcumin. *Toxicol. Rep.* **2021**, *8*, 1143–1155. [[CrossRef](#)]
11. Bangham, A.D.; Horne, R.W. Negative staining of phospholipids and their structural modification by surface-active agents as observed in the electron microscope. *J. Mol. Biol.* **1964**, *8*, 660–668. [[CrossRef](#)]
12. Allen, T.M.; Cullis, P.R. Liposomal drug delivery systems: From concept to clinical applications. *Adv. Drug Deliv. Rev.* **2013**, *65*, 36–48. [[CrossRef](#)]
13. Schmid, M.H.; Korting, H.C. Therapeutic progress with topical liposome drugs for skin disease. *Adv. Drug Deliv. Rev.* **1996**, *18*, 335–342. [[CrossRef](#)]
14. Elsayed, M.M.A.; Abdallah, O.Y.; Naggar, V.F.; Khalafallah, N.M. Deformable liposomes and ethosomes: Mechanism of enhanced skin delivery. *Int. J. Pharm.* **2006**, *322*, 60–66. [[CrossRef](#)]
15. Touitou, E.; Dayan, N.; Bergelson, L.; Godin, B.; Eliaz, M. Ethosomes—Novel vesicular carriers for enhanced delivery: Characterization and skin penetration properties. *J. Control. Release* **2000**, *322*, 60–66. [[CrossRef](#)]
16. Cristiano, M.C.; Froiio, F.; Mancuso, A.; Iannone, M.; Fresta, M.; Fiorito, S.; Celia, C.; Paolino, D. In vitro and in vivo trans-epidermal water loss evaluation following topical drug delivery systems application for pharmaceutical analysis. *J. Pharm. Biomed. Anal.* **2020**, *186*, 113295. [[CrossRef](#)]
17. Ainbinder, D.; Touitou, E. Testosterone ethosomes for enhanced transdermal delivery. *Drug Deliv. J. Deliv. Target. Ther. Agents* **2005**, *12*, 297–303. [[CrossRef](#)] [[PubMed](#)]
18. Ibaraki, H.; Kanazawa, T.; Oogi, C.; Takashima, Y.; Seta, Y. Effects of surface charge and flexibility of liposomes on dermal drug delivery. *J. Drug Deliv. Sci. Technol.* **2019**, *57*, 101754. [[CrossRef](#)]
19. Barone, A.; Cristiano, M.C.; Cilurzo, F.; Locatelli, M.; Iannotta, D.; Di Marzio, L.; Celia, C.; Paolino, D. Ammonium glycyrrhizate skin delivery from ultradeformable liposomes: A novel use as an anti-inflammatory agent in topical drug delivery. *Colloids Surf. B* **2020**, *193*, 111152. [[CrossRef](#)] [[PubMed](#)]
20. Mancuso, A.; Cristiano, M.C.; Fresta, M.; Paolino, D. The challenge of nanovesicles for selective topical delivery for acne treatment: Enhancing absorption whilst avoiding toxicity. *Int. J. Nanomed.* **2020**, *15*, 9197–9210. [[CrossRef](#)] [[PubMed](#)]
21. Kitagawa, S.; Kasamaki, M. Enhanced Delivery of Retinoic Acid to Skin by Cationic Liposomes. *Chem. Pharm. Bull.* **2006**, *54*, 242–244. [[CrossRef](#)]
22. Fresta, M.; Mancuso, A.; Cristiano, M.C.; Urbanek, K.; Cilurzo, F.; Cosco, D.; Iannone, M.; Paolino, D. Targeting of the pilosebaceous follicle by liquid crystal nanocarriers: In vitro and in vivo effects of the entrapped minoxidil. *Pharmaceutics* **2020**, *12*, 1127. [[CrossRef](#)]
23. Verma, P.; Pathak, K. Therapeutic and cosmeceutical potential of ethosomes: An overview. *J. Adv. Pharm. Technol. Res.* **2010**, *1*, 274–282. [[CrossRef](#)] [[PubMed](#)]
24. Li, G.; Fan, Y.; Fan, C.; Li, X.; Wang, X.; Li, M.; Liu, Y. Tacrolimus-loaded ethosomes: Physicochemical characterization and in vivo evaluation. *Eur. J. Pharm. Biopharm.* **2012**, *82*, 49–57. [[CrossRef](#)] [[PubMed](#)]
25. Hattori, Y.; Date, M.; Arai, S.; Kawano, K.; Yonemochi, E.; Maitani, Y. Transdermal Delivery of Small Interfering RNA with Elastic Cationic Liposomes in Mice. *J. Pharm.* **2013**, *2013*, 149695. [[CrossRef](#)]
26. Lin, H.W.; Xie, Q.C.; Huang, X.; Ban, J.F.; Wang, B.; Wei, X.; Chen, Y.Z.; Lu, Z.F. Increased skin permeation efficiency of imperatorin via charged ultradeformable lipid vesicles for transdermal delivery. *Int. J. Nanomed.* **2018**, *2018*, 831–842. [[CrossRef](#)]
27. Jung, S.; Otberg, N.; Thiede, G.; Richter, H.; Sterry, W.; Panzner, S.; Lademann, J. Innovative liposomes as a transfollicular drug delivery system: Penetration into porcine hair follicles. *J. Investig. Dermatol.* **2006**, *126*, 1728–1732. [[CrossRef](#)] [[PubMed](#)]
28. Cristiano, M.C.; Froiio, F.; Mancuso, A.; Cosco, D.; Dini, L.; Di Marzio, L.; Fresta, M.; Paolino, D. Oleuropein-laded ufasomes improve the nutraceutical efficacy. *Nanomaterials* **2021**, *11*, 105. [[CrossRef](#)]
29. Danaei, M.; Dehghankhold, M.; Atefi, S.; Hasanzadeh Davarani, F.; Javanmard, R.; Dokhani, A.; Khorasani, S.; Mozafari, M.R. Impact of Particle Size and Polydispersity Index on the Clinical Applications of Lipidic Nanocarrier Systems. *Pharmaceutics* **2018**, *10*, 57. [[CrossRef](#)]

30. Hoshyar, N.; Gray, S.; Han, H.; Bao, G. The effect of nanoparticle size on in vivo pharmacokinetics and cellular interaction. *Nanomedicine* **2016**, *11*, 673–692. [[CrossRef](#)]
31. Verma, D.D.; Verma, S.; Blume, G.; Fahr, A. Particle size of liposomes influences dermal delivery of substances into skin. *Int. J. Pharm.* **2003**, *258*, 141–151. [[CrossRef](#)]
32. Mota, A.H.; Rijo, P.; Molpeceres, J.; Reis, C.P. Broad overview of engineering of functional nanosystems for skin delivery. *Int. J. Pharm.* **2017**, *532*, 710–728. [[CrossRef](#)] [[PubMed](#)]
33. Limsuwan, T.; Boonme, P.; Khongkow, P.; Amnuakit, T. Ethosomes of Phenylethyl Resorcinol as Vesicular Delivery System for Skin Lightening Applications. *Biomed Res. Int.* **2017**, *2017*, 8310979. [[CrossRef](#)]
34. Paliwal, S.; Tilak, A.; Sharma, J.; Dave, V.; Sharma, S.; Yadav, R.; Patel, S.; Verma, K.; Tak, K. Flurbiprofen loaded ethosomes—Transdermal delivery of anti-inflammatory effect in rat model. *Lipids Health Dis.* **2019**, *18*, 133. [[CrossRef](#)] [[PubMed](#)]
35. Pilch, E.; Musiał, W. Liposomes with an ethanol fraction as an application for drug delivery. *Int. J. Mol. Sci.* **2018**, *19*, 3806. [[CrossRef](#)] [[PubMed](#)]
36. Cristiano, M.C.; Froiio, F.; Spaccapelo, R.; Mancuso, A.; Nisticò, S.P.; Udongo, B.P.; Fresta, M.; Paolino, D. Sulfuraphane-Loaded Ultradeflexible Vesicles as a Potential Natural Nanomedicine for the Treatment of Skin Cancer Diseases. *Pharmaceutics* **2020**, *12*, 6. [[CrossRef](#)] [[PubMed](#)]
37. Bos, J.D.; Meinardi, M. The 500 Dalton rule for the skin penetration of chemical compounds and drugs. *Exp. Dermatol.* **2000**, *9*, 165–169. [[CrossRef](#)] [[PubMed](#)]
38. Zhang, Y.; Jing, Q.; Hu, H.; He, Z.; Wu, T.; Guo, T.; Feng, N. Sodium dodecyl sulfate improved stability and transdermal delivery of salidroside-encapsulated niosomes via effects on zeta potential. *Int. J. Pharm.* **2020**, *580*, 119183. [[CrossRef](#)]
39. Andleeb, M.; Shoaib Khan, H.M.; Daniyal, M. Development, Characterization and Stability Evaluation of Topical Gel Loaded with Ethosomes Containing *Achillea millefolium* L. Extract. *Front. Pharmacol.* **2021**, *12*, 603227. [[CrossRef](#)]
40. Mandzy, N.; Grulke, E.; Druffel, T. Breakage of TiO<sub>2</sub> agglomerates in electrostatically stabilized aqueous dispersions. *Powder Technol.* **2005**, *160*, 121–126. [[CrossRef](#)]
41. Celia, C.; Trapasso, E.; Cosco, D.; Paolino, D.; Fresta, M. Turbiscan lab expert analysis of the stability of ethosomes and ultradeflexible liposomes containing a bilayer fluidizing agent. *Colloids Surf. B Biointerfaces* **2009**, *72*, 155–160. [[CrossRef](#)]
42. Wang, C.; Hong, H.H.; Chen, M.; Ding, Z.; Rui, Y.; Qi, J.; Li, Z.-C.; Liu, Z. Cationic Micelle as An In Vivo Catalyst for Tumor-Localized Cleavage Chemistry. *Angew. Chem. Int. Ed.* **2021**. online ahead of print. [[CrossRef](#)]
43. de Lima, M.; Neves, S.; Filipe, A.; Duzgunes, N.; Simoes, S. Cationic Liposomes for Gene Delivery: From Biophysics to Biological Applications. *Curr. Med. Chem.* **2003**, *10*, 1221–1231. [[CrossRef](#)]
44. Choi, J.S.; Lee, E.J.; Jang, H.S.; Park, J.S. New cationic liposomes for gene transfer into mammalian cells with high efficiency and low toxicity. *Bioconjug. Chem.* **2001**, *12*, 108–113. [[CrossRef](#)] [[PubMed](#)]
45. del Pozo-Rodríguez, A.; Delgado, D.; Solinís, M.A.; Gascón, A.R.; Pedraz, J.L. Solid lipid nanoparticles: Formulation factors affecting cell transfection capacity. *Int. J. Pharm.* **2007**, *339*, 261–268. [[CrossRef](#)] [[PubMed](#)]
46. Lv, H.; Zhang, S.; Wang, B.; Cui, S.; Yan, J. Toxicity of cationic lipids and cationic polymers in gene delivery. *J. Control. Release* **2006**, *114*, 100–109. [[CrossRef](#)] [[PubMed](#)]
47. Mohd Izhah, M.N.; Hussin, Y.; Aziz, M.N.M.; Yeap, S.K.; Rahman, H.S.; Masarudin, M.J.; Mohamad, N.E.; Abdullah, R.; Alitheen, N.B. Preparation and Characterization of Self Nano-Emulsifying Drug Delivery System Loaded with Citraland Its Antiproliferative Effect on Colorectal Cells In Vitro. *Nanomaterials* **2019**, *9*, 1028. [[CrossRef](#)] [[PubMed](#)]